VOL.40 Nº4 2023
https://doi.org/10.22491/rmct.v40i4.11950.en

Evaluation of micro-alloyed steels with low carbon and high mechanical strength, subjected to the Hardening and Partitioning process

Flávia Tolomelli[1],*, Andersan dos Santos Paula[1], Fernando Cosme Rizzo Assunção[2]
[1]Instituto Militar de Engenharia, Rio de Janeiro, RJ, Brasil
[2] Pontifícia Universidade Católica do Rio de Janeiro - PUC-RJ, Rio de Janeiro, RJ, Brasil
***flavia.tolomelli@ime.eb.br**

ABSTRACT: Quenching and partitioning can produce AHSS (advanced high strength steel) with good toughness and ductility. This study evaluated the performance of two alloys of these steel forms (with Ti or Cr addition) that were subjected to one-stage quenching and partitioning. This study used the ThermoCalc program (TCFE9) to determine austenite composition and empirical equations to determine the main transformation temperatures of interest in this process, which were used as a basis for quenching heat treatments in oil. The alloys were characterized by optical and scanning electron microscopy and phase quantification on Image J. The latter was used to indirectly evaluate the retained austenite content as a function of the MA constituent fraction (martensite-austenite). Results found that the alloy with Ti-addition showed higher fractions of MA and higher yield strength, tensile strength limit, and total elongation than than with Cr, indicating its greater aptitude for quenching and partitioning.

KEYWORDS: Microalloyed steels; Q&P; ThermoCalc; retained austenite.

RESUMO: Por meio do processo de têmpera e partição podem ser obtidos aços AHSS (Aços Avançados de Alta Resistência) com boa tenacidade e ductilidade. Neste trabalho é avaliado o desempenho de duas ligas desses aços (com adição de Ti ou Cr) submetidas ao processo de Têmpera e Partição (T&P) de um estágio. O estudo envolveu o uso do programa ThermoCalc (TCFE9) para determinar a composição da austenita, bem como equações empíricas para determinar as principais temperaturas de transformação de interesse nesse processo, usadas como base para os tratamentos térmicos de têmpera com resfriamento em óleo. A caracterização das ligas foi feita usando microscopia ótica e eletrônica de varredura, como também quantificação de fase com auxílio do software Image J. Esse último para avaliar de forma indireta o percentual de austenita retida em função da fração de constituinte MA (martensita-austenita). Como resultado foi observado que a liga com adição de Ti comparada à liga com adição de Cr além de apresentar maiores frações de MA, apresentou maiores valores de limite de escoamento, limite de resistência e alongamento total, indicando que ela apresenta maior aptidão ao processo T&P.

PALAVRAS-CHAVE: Aços microligados; T&P; ThermoCalc; Austenita retida.

1. Introduction[1]

The third generation of advanced high-strength steels (AHSS) are aimed at adding greater toughness and ductility to first-generation AHSS. This is possible because these steels contain a high volumetric fraction of fine-grained ferrite, carbide-free bainite, martensite, and retained austenite in their microstructure. The ultrafine-grained ferrite, bainite, and martensite constituents provide the level of mechanical strength, while the ductility and high strain-hardening exponent are highly dependent on the fraction and mechanical stability of the austenite (GRAJCAR, KUZIAK, ZALECKI, 2012; MATLOCK, SPEER, 2009). The concept behind the microstructure design of third-generation AHSS is to achieve a considerable amount of retained austenite (> 20% by volume) within a martensitic/ferritic matrix. To obtain this sophisticated multiphase structure, complex thermal processing routes are employed (BLECK et al., 2019). Thus, steels produced through the quenching and partitioning process (Q&P steels) stand out.

The quenching and partitioning process (Q&P process), initially proposed by Speer, has proven to be a viable route for obtaining steels with mixed microconstituents, making them attractive due

1 Observações iniciais ou contextualização, se necessárias, devem ser incluídas como nota de rodapé na in
Os títulos dos itens e subitens são apenas exemplos. No entanto, sugerimos usar o formato 1.2.3 para sua subdivisão.

to their excellent combination of properties with minimal alloying element addition (SEO, 2019). A good alloy design for producing quenching and partitioning steel with a microstructure consisting of martensite laths separated by thin films of retained austenite should consider the addition of alloying elements that, combined with the high cooling rates employed in the quenching process, allow what follows. These are: preventing of ferrite and pearlite phases during quenching; the delaying or inhibiting bainite formation; avoiding or minimizing carbide precipitation (which would consume the carbon needed to stabilize the austenite); and achieving a sufficiently high carbon content to stabilize a considerable fraction of retained austenite at room temperature (SANTOFIMIA, 2011). For this purpose, in addition to C, these steels contain other alloying elements such as Mn, Ni, and Cr, which delay the formation of ferrite, pearlite, and bainite; and Si, Al, or P, which, added individually or in combinations, inhibit the precipitation of epsilon carbides and cementite, which would consume the carbon necessary for austenite stability. Carbon enrichment of austenite is considered beneficial because the TRIP effect during deformation can significantly contribute to the steel formability and energy absorption capacity (SANTOFIMIA, 2008). Additionally, carbon and Mn, along with other gamma-stabilizing alloying elements, reduce the A_{c3} or A_{r3} temperature (i.e., eutectoid transformation or decomposition temperature [A_{e3}] outside equilibrium during cooling or heating, respectively), increasing the austenite stability field.

The Q&P process, shown in Figure 1, was proposed to create steel microstructures containing retained austenite and has been the subject of various research studies since then (SPEER, 2003). It consists of an initial soaking heat treatment, starting from either full austenitization (austenitic field) or partial austenitization (intercritical field) of the steel, followed by cooling at a rate that inhibits any diffusional or mixed transformation, interrupted at a temperature between M_i and M_f, i.e., the martensitic transformation start and finish temperatures, as shown in Figure 1. At the end of this stage of the process, the microstructure consists of controlled fractions of martensite and retained austenite. During the quenching time (Qt) at this temperature range (one-stage treatment) or at a temperature slightly above M_i (two-stage treatment), carbon partitioning occurs from the carbon-supersaturated martensite to the untransformed austenite, aiming to stabilize it by lowering its M_i' and M_f' temperatures (as shown in Figure 1), meaning that after final cooling, carbon-enriched austenite remains present down to room temperature.

Thus, the final volumetric fraction of austenite can be controlled by the interruption temperature of the quenching cooling between M_i and M_f. At the end of the treatment, microstructures consisting of martensite and retained austenite (if soak was conducted from the austenitic field) or free ferrite, martensite, and retained austenite (if soak was conducted from the intercritical field) are obtained (SPEER, 2005; SPEER, 2011).

Figure 1 - single-stage and two-stage Q&P process applied to Q&P-suitable steels. M_i and M_f = refer to retained austenite during quenching; $M_{i'}$ and $M_{f'}$ = refer to carbon-enriched austenite during partitioning.

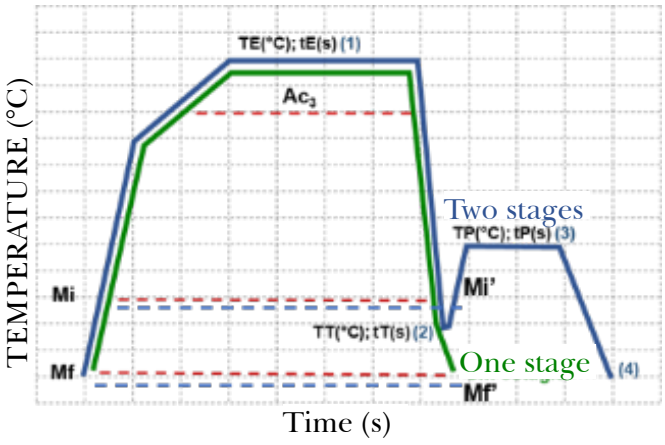

The factors influencing the volume fraction of retained austenite in Q&P steels primarily include the chemical composition, which determines the M_i temperature of austenite; the quenching temperature

(QT), which defines the initial volume fraction of martensite; and the partitioning time, which determine the final volume fraction of retained austenite. If the partitioning time is too short, the carbon diffusion from martensite to austenite will be insufficient, causing the retained austenite to become unstable and transform into martensite during the subsequent cooling process. If the partitioning time is too long, the retained austenite will become enriched in carbon but may decompose into ferrite and carbide or into bainite at the partitioning temperature (PT), reducing the volume fraction of retained austenite (WANG, SPEER, 2013; TOJI, MIYAMOTO, RAABE, 2015; KIM et al., 2009; LI et al., 2010; DE MOOR et al., 2006).

Other factors include the austenitic grain size and austenite morphology. The carbon percentage of austenite is affected by the partitioning time and temperature, such that increasing both the time and temperature of partitioning will increase the carbon diffusion rate and, consequently, the stabilization of retained austenite (KNIF et al., 2014; XIE et al., 2019; ZINSAS-BORUJERDI et al., 2018; ZHAO et al., 2014).

Regarding mechanical properties, according to Zinsaz-Borujerdi et al. (2018), the volume fraction of retained austenite in steels subjected to the Q&P process is considered the main factor affecting ductility, i.e., the total elongation evaluated in a uniaxial tensile test. The primary reason for this is that the total elongation of the steel depends not only on the percentage of retained austenite but also on its carbon content. This is because the stability of carbon-enriched austenite at the end of the soak at partitioning temperature determines whether, in the subsequent cooling, there will be only retained austenite alongside tempered martensite or retained austenite combined with additional martensite with higher carbon content along with some retained austenite. Increasing the partitioning time or temperature raises the carbon diffusion rate and, consequently, the stability of retained austenite (ZHAO et al., 2014). Matsumura, Sakuma, and Takechi (1987) concluded that the higher the percentage and stability of retained austenite, the greater the total elongation obtained.

Various studies have shown the influence of processing conditions of Q&P steels and their microstructures on the results of mechanical properties (JUNG, 2011; ARLAZAROV et al., 2016; KICKINGER et al., 2021; CHENG et al., 2022; JING, 2014; HE et al., 2019).

The objective of this work was to evaluate two AHSS microalloyed steels with different compositions, regarding their suitability for producing Q&P steel when subjected to a one-step Q&P process. After obtaining the microstructures resulting from the proposed Q&P process, their characterization was performed using optical and scanning electron microscopy, based on prior contrast using Klemm's color etching solution and the conventional 3% Nital reagent, respectively. This allowed the identification of the microconstituents through image analysis of the optical microscopy micrographs, as well as the quantification of retained austenite through the estimation of the MA constituent percentage using ImageJ software. These results were further complemented by mechanical characterization through uniaxial tensile testing.

2. Materials and Methods Method

2.1. Alloy design determination

The selection of alloys, aiming to evaluate the suitability of the steels for the Q&P process, considered a basic chemical composition of Fe-C-Mn-Si for two microalloyed Nb steels, with Alloy A containing additions of Ti and Mo, and Alloy B with additions of Cr and Mo, as shown in Table 1. The alloys were cast on an industrial scale in an LD converter, and after the hot rolling, pickling, and cold rolling processes, samples were taken from the sheets for this study.

Table 1 - Chemical composition (%wt) of the alloys selected for the study. Source: X

Alloys	C	Mn	Cr	Si	Mo	Ti+nB
Alloy A	0.15	2.0	-	0.5	0.3	.1
Alloy B	0.20	2.0	0.3	0.5	0.3	0.050
(maximum values).						

2.2. Determination of soaking temperatures for quenching treatment

The ThermoCalc software, using the TCFE9 database version, was used to determine temperatures that define the intercritical region in equilibrium (Ae1 and Ae3), evaluate the chemical composition of austenite (carbon percentage), and the precipitation temperatures of phases from the austenitic region.

2.2.1. Empirical equations

Empirical equations (GORNI, 2019) for determining A_{c1}, A_{c3}, and M_i temperatures were adopted as indicated in equations 1, 2, and 3, They were then compared with the obtained values using ThermoCalc. These temperatures were used as the basis for the proposed quenching heat treatments in this work for the one-step Q&P process.

$$Ac_1 = 739 - 22{,}8C - 6{,}8Mn + 18{,}2Si + 11{,}7Cr - 15Ni - 6{,}4Mo - 5V - 28Cu \quad \text{Equation 1.}$$

$$Ac_3 = 937{,}3 - 224{,}5C - 17Mn + 34Si - 14Ni + 21{,}6Mo + 41{,}8V - 20Cu \quad \text{Equation 2.}$$

$$M_i = 539 - 423C - 30{,}4Mn - 17{,}7Ni - 12{,}1Cr - 11Si - 7{,}5Mo \quad \text{Equation 3.}$$

2.3 Sampling for heat treatments

Cold-rolled sheets with a thickness of 1.50 mm, produced on an industrial scale, were collected, and test specimens prepared with dimensions of 90 x 270 mm (longitudinal direction – LD in relation to the rolling direction) for conducting heat treatments. The one-step Q&P process with different soaking temperatures for each steel was carried out in a muffle furnace, with temperature monitoring through K-type thermocouples attached to the sheets and connected to a Fluke device.

2.4. One-step Q&P process

For the quenching and partitioning heat treatments, two soaking conditions were used: soaking in the austenitic field and soaking in the intercritical field, due to the proposed one-step Q&P process. For soaking in the austenitic field, a temperature of 840°C was adopted for both alloys of the study, as the A_{c3} temperatures of the alloys were below this temperature. For the intercritical field heat treatment, based on the A_{c1} and A_{c3} temperatures obtained, temperatures of 780°C and 820°C with a soaking time of 120 s and a hold time of 20 s were used. The cooling medium was room temperature oil, and the cooling rate achieved was over 20°C/s. An example of a graph obtained for monitoring the thermal cycle profile during the heat treatments can be seen in Figure 2. It shows that heating occurred with a non-linear profile and a decreasing rate as temperature increased, subdivided into two regions: preheating (average rate of 10°C/s) and heating (lower rate with more variation). Thus, the sheets required a hold time of approximately 90 seconds in the preheated furnace at the proposed soaking temperature before the soaking time could be considered.

Figure 2 - Heat treatment scheme used for Alloys A and B.

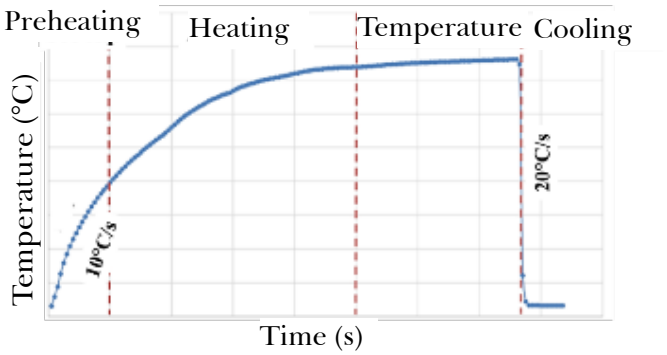

2.5. Metallographic characterization

Two techniques were used for metallographic characterization, as follows.

a. Optical microscopy (OM) – using a Zeiss microscope – with conventional reagents based on Nital (3 mL of nitric acid diluted in 97 mL of ethanol) and Klemm (aqueous saturated solution of sodium thiosulfate: 50 mL (solubility of anhydrous sulfate (Na2S2O3) 50 g/100 mL at 20°C, hydrated sulfate solubility 291.1 g/100 mL at 45°C, and 1 g of potassium metabisulfite). Etching time varied depending on the microstructure;
b. Scanning electron microscopy (SEM) – QUANTA 3D FEG – based on the microstructures revealed with the Nital 3% solution.

2.6. Quantitative metallography

To conduct an estimated quantitative evaluation of the retained austenite fraction present in the microstructure and associated with the MA constituent percentage, the ImageJ software was used as a tool to aid the characterization. Two test specimens from each alloy, subjected to the same treatment conditions, were used for a comparative analysis of the microstructures resulting from the Nital 3% etching.

2.7. Mechanical characterization

Uniaxial tensile tests were conducted on an Instron 5585H 25t machine, with total elongation determined by an AVE video extensometer. A total of two test specimens per condition under study for each alloy were taken from the longitudinal position and followed the ASTM-E-290 standard, being of the ISO I type with a 50 mm gauge length.

3. Results and Discussions

3.1 Thermodynamic aspects

In Figure 3 (a,b), the A_{e1} and A_{e3} temperatures, calculated via Thermocalc for alloys A and B, can be observed, showing a larger stability field for austenite in the first alloy compared to the second. In Figure 4 (a,b), the precipitation temperatures of carbides, nitrides, and carbonitrides for the respective alloys are shown. It is noted that, under equilibrium conditions, alloy A may consume more carbon in the formation of precipitates (08 carbon-based precipitates) than alloy B (05 carbon-based precipitates), indicating that in the latter, there is a greater likelihood of excess carbon available to stabilize austenite at room temperature compared to the former.

Figure 3 - Graphs related to thermodynamic data of Alloy A under equilibrium conditions, highlighting: (a) the phase transformation temperatures, A_{e1} and A_{e3}, and the distribution of carbon in austenite; and (b) the phase maps.

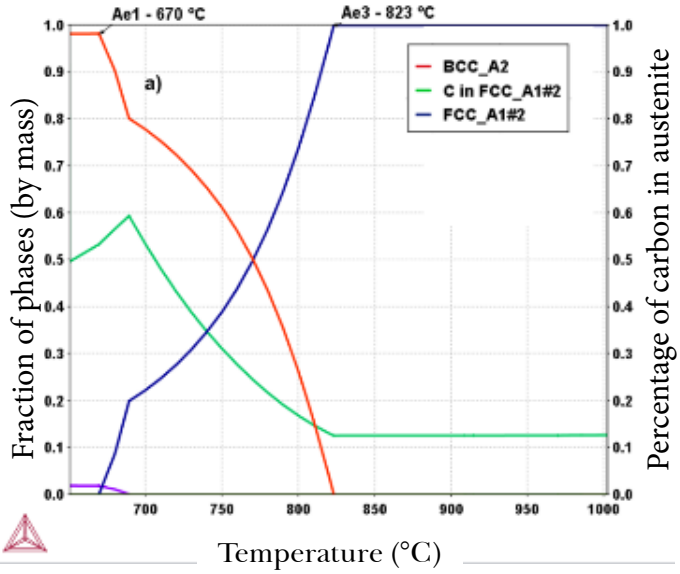

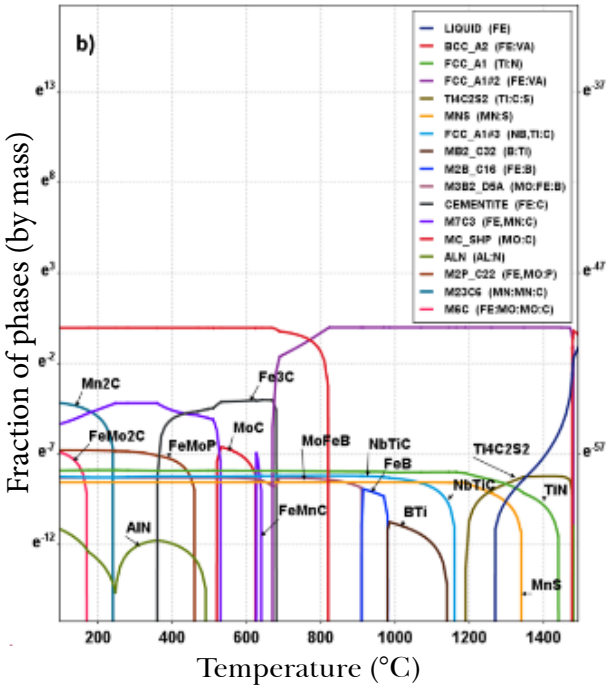

Figure 4 - Graphs related to thermodynamic data of Alloy B under equilibrium conditions, highlighting: (a) the phase transformation temperatures, Ae1 and Ae3, and the distribution of carbon in austenite; and (b) the phase maps.

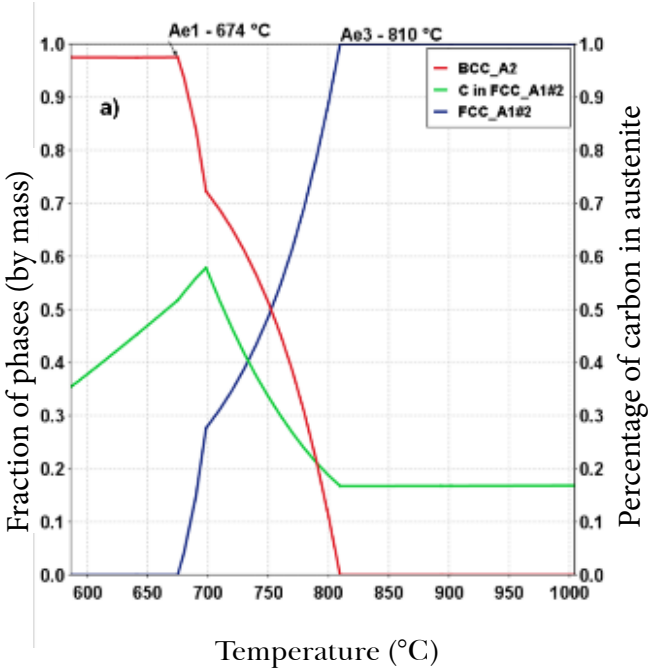

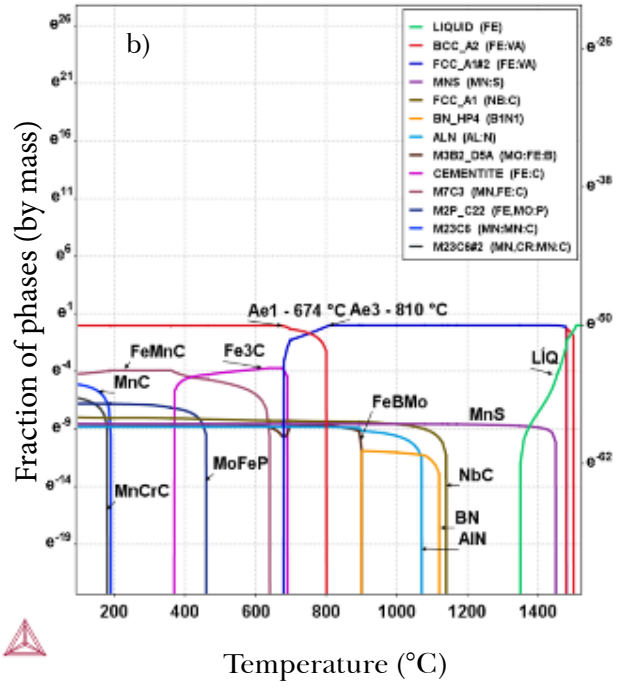

3.2 Carbon Percentage in Austenite and CE

For alloy A it can be seen in Figure 3(a) that the carbon percentages in austenite (under equilibrium conditions) are above 0.20 %C at 780 °C and below 0.15 %C at 820 and 840 °C. And for alloy B it can be seen in Figure 4 (a) that these values remained above 0.20 %C at the temperature of 780 °C but remained above 0.15 %C at the temperatures of 820 and 840 °C, respectively.

In Table 2, it can be observed that the carbon equivalent content of alloy A (0.71; 0.52; 0.52%) is lower than that of alloy B (0.73; 0.60; 0.60%), respectively at the temperatures 780°C, 820°C, and 840°C, indicating that alloy B may exhibit greater hardenability compared to alloy A.

Table 2 - Carbon equivalent percentage of alloys A and B at different soaking temperatures.

	Carbon equivalent percentage of alloys	
T(°C)	Alloy A	Alloy B
780	0.71	0.73
820	0.52	0.60
840	0.52	0.60

3.3 Microstructural evaluation

Figures 5, 6, and 7 present the microstructural aspects resulting from the quenching heat treatment, performed in the intercritical field at soaking temperatures of 780°C and 820°C, and in the austenitic field at a soaking temperature of 840°C, respectively. The soaking time was of two minutes, based on analyses performed with optical microscopy (OM) and scanning electron microscopy (SEM).

Figure 5 - Microstructural characterization: OM (500x) and SEM (20,000x), and their results (estimate) of retained austenite quantification (related to the MA constituent) for alloys A and B subjected to the Q&P process, with soak at 780 °C.

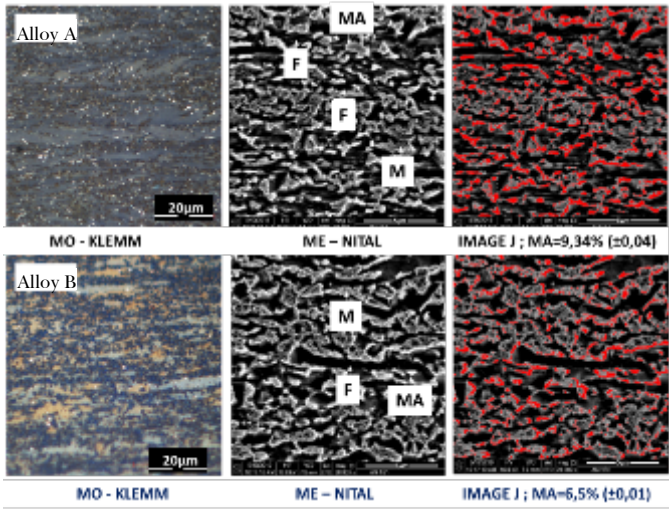

The micrographs from the microstructural analysis are displayed in Figures 5, 6, and 7, from left to right as follows. Optical microscope micrograph resulting from the colored etching with Klemm's solution (first column). Scanning electron microscope micrograph resulting from the etching with 3% Nital solution (second column). And the respective image analysis for retained austenite quantification using ImageJ (third column), based on the selection of lighter regions highlighted in the SEM micrographs.

Figure 6 - Microstructural characterization: OM (500x) and SEM (20,000x), and their results (estimate) of retained austenite quantification (related to the MA constituent) for alloys A and B subjected to the T&P process, with soak at 820 °C.

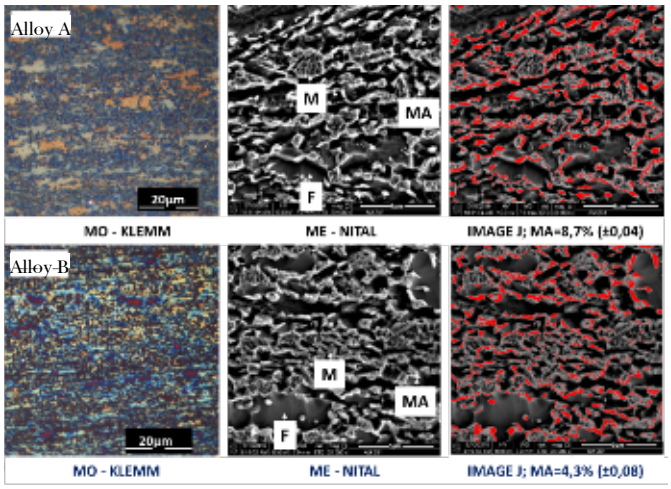

Figure 7 - Microstructural characterization: OM (500x) and SEM (20,000x), and their results (estimate) of retained austenite quantification (related to the MA constituent) for alloys A and B subjected to the T&P process, with soaking at 840 °C.

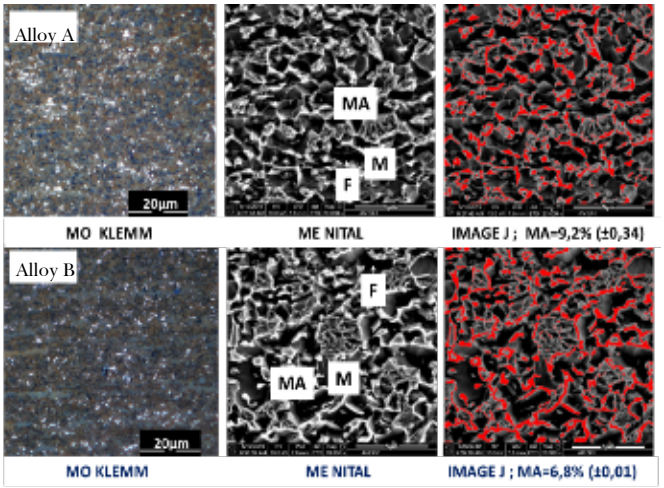

When comparing the quantification of samples treated at 780 °C, 820 °C, and 840 °C, a slight reduction in the retained austenite percentage (re-

lated to the MA constituent) was observed as the soaking temperature increased from 780 °C to 820 °C. This may be associated with the decrease in the carbon percentage in the alloys from 0.20%C at 780°C to 0.14%C at 820°C for alloy A, and from 0.25%C at 780°C to <0.15%C for alloy B, as seen with the increasing treatment temperature. This reduces the possibility of retained austenite stability at room temperature due to the decrease in M_f temperature and a higher proportion of austenite in the MA constituent.

It was also observed that alloy A exhibited a higher percentage of retained austenite (estimated by the MA constituent percentage) compared to alloy B at 840 °C. In this temperature range, the carbon percentage in the austenite matches the carbon percentage in the alloys, i.e., 0.13%C for alloy A and >0.15%C for alloy B.

3.4. Tensile test

Table 3 presents the mechanical properties (average of two test specimens) for the variables of yield strength, YS (MPa), ultimate tensile strength, UTS (MPa), total elongation, TE (%), and strain hardening exponent, n-value (measured up to a maximum of 6% strain). Alloy B, treated at 820 ° was an exception, in which measurement was taken up to 4% strain), extracted from uniaxial tensile tests conducted on specimens for the two alloys studied, treated at temperatures of 780, 820, and 840 °C (as shown in Figure 8), with these values correlated with the MA constituent percentages quantified in the metallographic analysis.

Table 3 - Results of mechanical properties of alloys A and B, correlated with the MA constituent fraction as a function of the heat treatment temperature.

Ligas	Temp°C) LE	(Mpa) LR	(Mpa)	Al (%)	$N_{4-6\%}$	MA (%)
A	780	804	1309	9.4	0.15	9.34 ± 0.2
B	780	670	1270	7.7	0.17	6.5 ± 0.3
A	820	760	1306	6.5	0.12	8.7 ± 0.1
B	820	592	1199	4.1	0,09	4.3 ± 0.2
A	840	639	1100	13.9	0.19	9.2 ± 0.25
B	840	631	1152	6.5	0.19	6.8 ± 0.3

The results obtained highlight that Alloy A, by presenting higher values of MA constituent fraction (average of 10 measurements), also showed superior values for yield strength (LE, MPa), tensile strength (LR, MPa), and total elongation (AL, %) when treated at temperatures of 780 °C and 820 °C. However, the specimens resulting from heat treatment at 840 °C for both alloys showed a decrease in LE (MPa) and LR (MPa) values, while maintaining higher AL (%) for Alloy A. Finally, the n4-6% values did not show a conclusive behavior based on the alloys under study, soak temperatures during the quenching heat treatment, and the observed MA constituent fraction

Figure 8 - Engineering stress-strain curves for alloys A and B subjected to the Q&P process with soak temperatures of 780 °C (a), 820 °C (b) (intercritical range), and 840 °C (c) (austenitic range).

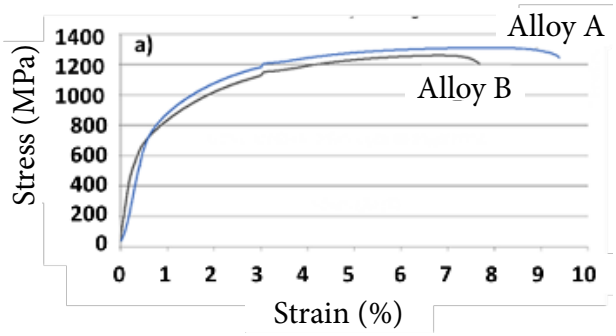

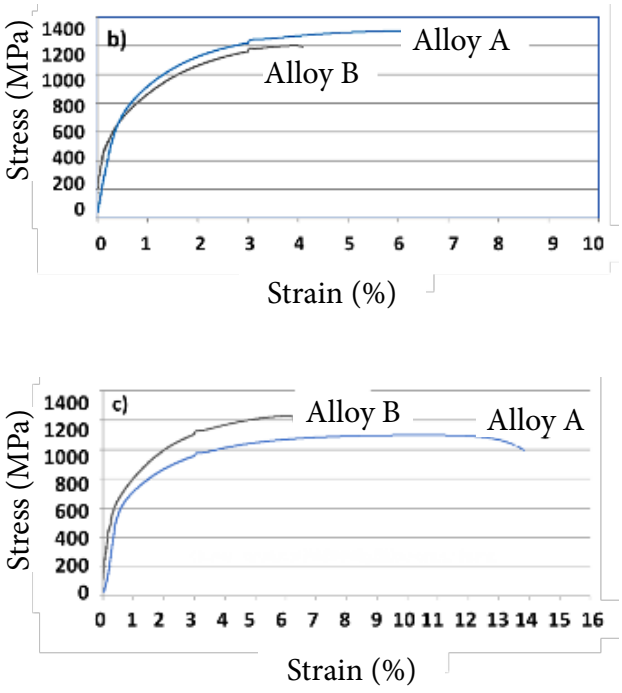

From the analysis of the engineering stress--strain curves shown in Figure 8, it is more evident that the increase in soak temperature used in the treatments resulted in a continuous improvement in total elongation and toughness for Alloy A compared to Alloy B, for the soak time applied in the treatment (2 minutes).

3.5. Influence of retained austenite percentage (related to the ma constituent) on total elongation

Figure 9 shows the quantified values of the MA constituent, related to retained austenite, with the total elongation observed in the specimens submitted to the uniaxial tensile test, after being subjected to the quenching heat treatments at the soaking temperatures of 780, 820 and 840 °C.

The trendline in the graph in Figure 9 shows that higher total elongation values tend to be obtained as the percentage of retained austenite, associated with the MA constituent, increases.

Figure 9 - Influence of retained austenite percentage (related to the % of MA constituent) on the total elongation of alloys A and B when subjected to a one--step T&P process.

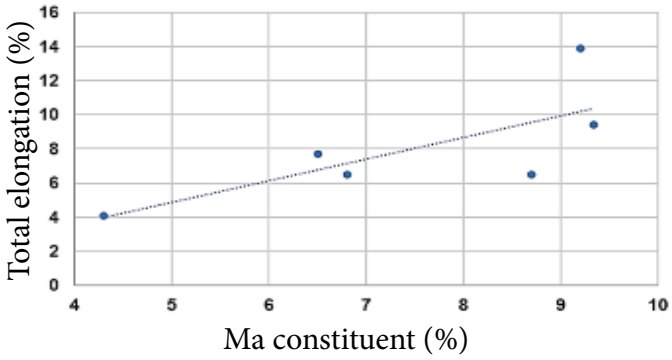

4. Conclusion

Regarding the suitability for the Q&P process (with soak in the intercritical and austenitic fields during quenching), it is concluded that the factors that may justify the microstructural evolution and distinct mechanical behavior between the alloys evaluated in this study can be associated with what follows.

a. The action of Ti combining with N at high temperatures, forming the TiN compound and likely leaving B in solid solution, which delays the austenite transformation process during cooling. This can be more clearly observed at the temperatures practiced in the intercritical field (780°C and 820°C).
b. Although during cooling the percentage of carbon in the alloy with Cr addition was more favorable for the stabilization of austenite, during heating, the dissolution of precipitates in this alloy may not have occurred throughout the soaking phase, alongside the recrystallization process of this alloy.
c. It is also likely that, from a kinetic perspective, there was less carbide formation in the alloy with Ti addition compared to the alloy with Cr addi-

tion, leaving more carbon free for austenite stabilization during cooling.

d. Therefore, it can be inferred that the alloy with Ti addition possibly indicates greater suitability for the Q&P process compared to the alloy with Cr addition, under the treatment conditions adopted in this study. This is due to the presentation of higher values in mechanical properties (YS, UTS, and El) and a greater percentage of MA constituent, as well as likely greater austenite retention at the end of the quenching cooling phase.

Acknowledgements

The authors would like to thank CSN, IME and PUC-RJ for the support received with the samples, laboratory tests and characterization, as well as PROEX/CAPES for the funding subsidies provided to PPGCM/IME.

References

[1] ARLAZAROV, A.; OLLAT, M.; MASSE, J. P.; BOUZAT, M. Influence of partitioning on mechanical behavior of Q&P steels. *Materials Science and Engineering: A*, [*s. l.*], v. 661, p. 79-86, 2016. DOI: 10.1016/j.msea.2016.02.071.

[2] ASTM INTERNATIONAL. *E290-14: Standard test methods for bend testing of material for ductility*. [*s. l.*]. 2014.

[3] BLECK, W.; BRÜHL, F.; MA, Y.; SASSE, C. Materials and processes for the third-generation advanced high--strength steels. *Berg- und Hüttenmännische Monatshefte*, [*s. l.*], v. 164, p. 466-474, 2019. DOI: 10.1007/s00501-019-00904-y.

[4] CHENG, Y. Y.; ZHAO, G.; XU, D. M.; MAO, X. P.; BAO, S. Q.; YANG, G. W. Comparative study on microstructures and mechanical properties of Q&P steels prepared with hot-rolled and cold-rolled C–Si–Mn sheets. *Journal of Materials Research and Technology*, [*s. l.*], v. 20, p. 1226-1242, 2022. DOI: 10.1016/j.jmrt.2022.07.139.

[5] CLARKE, A. J.; SPEER, J. G.; MATLOCK, D. K.; RIZZO, F. C.; EDMONDS, D. V.; SANTOFIMIA, M. J. Influence of carbon partitioning kinetics on final austenite fraction during quenching and partitioning. *Scripta Materialia*, [*s. l.*], v. 61, n. 2, p. 149-152, 2009. DOI: 10.1016/j.scriptamat.2009.03.02.1.

[6] DE MOOR, E.; LACROIX, S.; SAMEK, L.; PENNING, J.; SPEER, J. Dilatometric study of the quench and partitioning process. *In*: INTERNATIONAL CONFERENCE ON ADVANCED STRUCTURAL STEELS, 3., 2006, Gyeongju. *Proceedings Of The 3rd International Conference On Advanced Structural Steels*. Gyeongju: Korean Institute of Metals and Matereials, 2006.

[7] EDMONDS, D. V.; HE, K.; RIZZO, F. C.; DE COOMAN, B. C.; MATLOCK, D. K.; SPEER, J. G. Quenching and partitioning martensite — A novel steel heat treatment. *Materials Science and Engineering: A*, [*s. l.*], v. 438-440, p. 25-34, 2006. DOI: 10.1016/j.msea.2006.02.133.

[8] GORNI, A. A. *Steel forming and heat-treating handbook*. [*s. l.*]: [*s. n.*], 2019.

[9] GRAJCAR, A.; KUZIAK, R.; ZALECKI, W. Third generation of AHSS with increased fraction of retained austenite for the automotive industry. *Archives of civil and mechanical engineering*, [s. l.], v. 12, n. 3, p. 334-341, 2012.

[10] HE, J.; HAN, G.; LI, S.; ZOU, D. To correlate the phase transformation and mechanical behavior of QP steel sheets. *International Journal of Mechanical Sciences*, [*s. l.*], v. 152, p. 198-210, 2019.

[11] KICKINGER, C.; SUPPAN, C.; HEBESBERGER, T.; SCHNITZER, R.; HOFER, C. Microstructure and mechanical properties of partially ferritic Q&P steels. *Materials Science and Engineering: A*, [*s. l.*], v. 815, p. 141-296, 2021.

[12] KIM, D. H.; SPEER, J. G.; KIM, H. S.; DE COOMAN, B. C. Observation of an isothermal transformation during quenching and partitioning processing. *Metallurgical and Materials Transactions A*, [*s. l.*], v. 40, p. 2048-2060, 2009.

[13] KNIF, D. D.; PETROV, R.; FÖJER, C.; KESTENS, L. A. I. Effect of fresh martensite on the stability of retained austenite in quenching and partitioning steel. *Materials Science Engineering: A*, [*s. l.*], v. 615, p. 107-115, 2014. DOI: 10.1016/j.msea.2014.07.054.

[14] LI, H. Y.; LU, X. W.; LI, W. J.; JIN, X. J. Microstructure and mechanical properties of an ultrahigh-strength 40SiMnNiCr steel during the one-step quenching and partitioning process. *Metallurgical and Materials Transactions A*, [*s. l.*], v. 41, n. 5, p. 1284-1300, 2010. DOI: 10.1007/s11661-010-0184-8.

[15] LIU, H.; JIN, X.; DONG, H.; SHI, J. Martensitic microstructural transformations from the hot stamping, quenching and partitioning process. *Materials characterization*, [*s. l.*], v. 62, n. 2, p. 223-227, 2011.

[16] MATLOCK, D. K.; SPEER, J. G. Third generation of AHSS: microstructure design concepts. *In:* HALDAR, A.; SUWAS, S.; BHATTACHARJEE, D. (eds). *Microstructure and Texture in Steels and Other Materials*. Londres: Springer, 2009. p. 185-205.
[17] MATSUMURA, O.; SAKUMA, Y.; TAKECHI, H. Enhancemente of elongation by retained austenite in intercritical annealed 0,4C-1,5Si-0,8Mn steel. *Transaction ISIJ*, [*s. l.*], v. 27, n. 7, p. 570-579, 1987.
[18] SANTOFIMIA, M. J.; ZHAO, L.; PETROV, R.; SIETSMA, J. Characterization of the microstructure obtained by the quenching and partitioning process in a low-carbon steel. *Materials Characterization*, [*s. l.*], v. 59, n. 12, p. 1758-1764, 2008.
[19] SANTOFIMIA, M. J.; ZHAO, L.; PETROV, R.; KWAKERNAAK, C.; SLOOF, W.G.; SIETSMA, J. Microstructural development during the quenching and partitioning process in a newly designed low-carbon steel. *Acta Materialia*, [*s. l.*], v. 59, n. 15, p. 6059-6068, 2011.
[20] SEO, E. J.; CHO, L.; KIM, J. K.; MOLA, J.; ZHAO, L.; DE COOMAN, B. C. Constituent-specific properties in quenching and partitioning (Q&P) processed steel. *Materials Science and Engineering: A*, [*s. l.*], v. 740-741, p. 439-444, 2019.
[21] SPEER, J. G.; ASSUNÇÃO, F. C. R.; MATLOCK, D. K.; EDMONDS, D. V. The "quenching and partitioning" process: background and recent progress. *Materials Research*, [*s. l.*], v. 8, n. 4, p. 417-423, 2005. DOI: 1590/S1516-14392005000400010.
[22] SPEER, J. G.; DE MOOR, E.; FINDLEY, K. O.; MATLOCK, D. K.; DE COOMAN, B. C.; EDMONDS, D. V. Analysis of microstructure evolution in quenching and partitioning automotive sheet steel. *Metallurgical and materials transactions A*, [s. l.], v. 42, p. 3591-3601, 2011.
[23] SPEER, J. G.; STREICHER, A. M.; MATLOCK, D. K.; RIZZO, F.; KRAUSS, G. Quenching and partitioning: a fundamentally new process to create high strength trip sheet microstructures. *In*: SYMPOSIUM ON THE THERMODYNAMICS, KINETICS, CHARACTERIZATION AND MODELING, 2003, Chicago. *Austenite formation and decomposition*. Warrendale: TMS, 2003. p. 505-522.
[24] SUN, J.; YU, H. Microstructure development and mechanical properties of quenching and partitioning (Q&P) steel and an incorporation of hot-dipping galvanization during Q&P process. *Materials Science and Engineering: A*, [*s. l.*], v. 586, p. 100-107, 2013.
[25] SUN, J.; YU, H.; WANG, S.; FAN, Y. Study of microstructural evolution, microstructure-mechanical properties correlation and collaborative deformation-transformation behavior of quenching and partitioning (Q&P) steel. *Materials Science and Engineering A*, [*s. l.*], v. 596, p. 89-97, 2014.
[26] TOJI, Y.; MIYAMOTO, G.; RAABE, D. Carbon partitioning during quenching and partitioning heat treatment accompanied by carbide precipitation. *Acta Materialia*, [*s. l.*], v. 86, p. 137-147, 2015.
[27] WANG, L.; SPEER, J. G. Quenching and partitioning steel heat treatment. *Metallography, Microstructure, and Analysis*, [*s. l.*], v. 2, p. 268-281, 2013. DOI: 10.1007/s13632-013-0082-8.
[28] ZHAO, C. *et al*. Effect of annealing temperature and time on microstructure evolution of 0,2C-5Mn steel during intercritical annealing process. *Materials Science Technology*, [*s. l.*], v. 30, n. 7, p. 791-799, 2014. DOI: 10.1179/1743284713Y.0000000416.
[29] ZINSAZ-BORUJERDI, A.; ZAREI-HANZAKI, A.; ABEDI, H. R.; KARAM-ABIAN, M.; DING, H.; HAN, D.; KHERADMAN, N. Room temperature mechanical properties and microstructure of a low alloyed TRIP-assisted steel subjected to one-step and two-step quenching and partitioning process. *Materials Science and Engineering: A*, [*s. l.*], v. 725, p. 341-349, 2018.
[30] XIE, Z. J.; HAN, G.; YU, Y. S.; SHANG, C. J.; MISRA, R. D. K. The determining role of intercritical annealing condition on retained austenite and mechanical properties of a low carbon steel: Experimental and theoretical analysis. *Materials Characterization*, [*s. l.*], v. 153, p. 208-214, 2019. DOI: 10.1016/j.matchar.2019.05.010